Development 117, 873-883 (1993)
Printed in Great Britain © The Company of Biologists Limited 1993

Characterization of the unusually rapid cell cycles during rat gastrulation

Alasdair Mac Auley[1,*], Zena Werb[2] and Philip E. Mirkes[1]

[1]Department of Pediatrics, University of Washington, Seattle, WA 98195, USA
[2]Laboratory of Radiobiology and Environmental Health, University of California, San Francisco, CA 94143-0750, USA

*Author for correspondence (at address 2)

SUMMARY

The onset of gastrulation in rodents is associated with the start of differentiation within the embryo proper and a dramatic increase in the rate of growth and proliferation. We have determined the duration of the cell cycle for mesodermal and ectodermal cells of rat embryos during gastrulation (days 8.5 to 9.5 of gestation) using a stathmokinetic analysis. These embryonic cells are the most rapidly dividing mammalian cells yet described. Most cells of the ectoderm and mesoderm had a cell cycle time of 7 to 7.5 hours, but the cells of the primitive streak divided every 3 to 3.5 hours. Total cell cycle time was reduced by shortening S and G_2, as well as G_1, in contrast to cells later in development, when cell cycle duration is modulated largely by varying the length of G_1. In the ectoderm and mesoderm, G_1 was 1.5 to 2 hours, S was 3.5 to 4 hours, and G_2 was 30 to 40 minutes. G_1, S and G_2 were shortened even further in the cells of the primitive streak: G_1 was less than 30 minutes, S was 2 to 2.75 hours, and G_2 was less than 20 minutes. Thus, progress of cells through all phases of the cell cycle is extensively modified during rodent embryogenesis. Specifically, the increased growth rate during gastrulation is associated with radical changes in cell cycle structure and duration. Further, the commitment of cells to become mesoderm and endoderm by entering the primitive streak is associated with expression of a very short cell cycle during transit of the primitive streak, such that developmental decisions determining germ layer fate are reflected in differences in cell cycle regulation.

Key words: cell cycle, gastrulation, growth regulation, rodent, mesoderm, ectoderm, primitive streak

INTRODUCTION

Growth and cell proliferation are tightly controlled developmental processes. The final size and shape of an organism represents the interaction between growth and differentiation. Growth is the product of both cell division and mass increase, and cells need to integrate both for normal development. Most eukaryotic cells regulate their growth largely, if not exclusively, in G_1, prior to the onset of DNA synthesis, monitoring both their internal and external environments (reviewed by Pardee, 1989). S and G_2 show less variation in length, and progression through these phases of the cell cycle is relatively independent of changes in a cell's environment. Although most growth regulation in eukaryotes follows this pattern, there are a number of well-characterized exceptions, in which all phases of the cell cycle are subject to change. All the exceptions described occur during embryogenesis and may be the most direct pathway to link proliferation and development. The importance of close integration of growth and development suggests that direct modulation of the cell cycle by developmental pathways that regulate differentiation may be very common in the early embryogenesis of many species, including mammals.

During early embryonic development in *Xenopus laevis* and *Drosophila melanogaster*, progress through all phases of the cell cycle is extensively modified, and major developmental transitions are marked by changes in cell cycle regulation. In both species, the early cleavages immediately following fertilization are very rapid, containing only S phase and mitosis, with no detectable G_1 or G_2 phases (Rabinowitz, 1941; Graham and Morgan, 1966; Newport and Kirschner, 1982). The controls that normally operate in G_1 or G_2 appear to be overridden or irrelevant. At the midblastula transition, the cell cycle time slows dramatically in both species (Foe, 1989 and references therein; Graham and Morgan, 1966; Newport and Kirschner, 1982). In *Drosophila*, the three cell cycles following the midblastula transition are composed of S, G_2 and M phases (as cited by Edgar and O'Farrell, 1989). The length of G_2 is regulated by the product of *string*, the *Drosophila* homologue of the *Schizosaccharomyces pombe* cell division control gene *cdc25* (Edgar and O'Farrell, 1989; Russell and Nurse, 1986). Expression of *string* drives entry into mitosis and appears to be controlled in turn by the products of genes that control development (Edgar and O'Farrell, 1989; Foe and Odell, 1989). The coordination of *string* expression and hence division results in an exquisitely choreographed pattern of mitoses during these three cycles that reflects developmental fates for the cells (Foe, 1989; Foe

and Odell, 1989; Arora and Nusslein-Volhard, 1992). During subsequent development in *Drosophila*, the cells express cycles that contain G_1 in addition to S and G_2, and much of the growth regulation appears to occur in G_1 (Edgar and O'Farrell, 1990; reviewed by Glover, 1991, and O'Farrell et al., 1989).

The study of growth regulation during mammalian development has been considerably more limited and has focussed largely on later stages of development. Regulation of growth in the intestinal crypt appears to be a good model for much of the growth regulation that occurs during these later stages. The most rapid cell cycles in the crypt are 11 to 12 hours, divided as follows: G_1=2.5 to 4 hours; S=6.5 to 8 hours; G_2=1.5 to 2 hours; M=1 hour (Loeffler et al., 1986; reviewed by Potten and Loeffler, 1990). As the cells migrate out of the crypt and differentiate, the cell cycle lengthens progressively. The slowing of the cell cycle is achieved by lengthening G_1, with very little change in S, G_2 or M. Similar cell cycles are seen in rapidly growing cells in other mature tissues, and again cell cycle regulation is confined largely to G_1 (Cikes, 1970; Tobey et al., 1967). Eukaryotic cells can also be arrested in G_2, in response to either incomplete DNA synthesis or failure to repair DNA damage (Tobey, 1975; Downes et al., 1990; reviewed by Hartwell and Weinert, 1989). G_2 arrest appears to function more in damage control than growth control, requiring completion of DNA synthesis and repair so that the cells can progress through mitosis without sustaining irreparable damage (Hartwell and Smith, 1985; Hittelman and Rao, 1974a,b; Lau and Pardee, 1982; Weinert and Hartwell, 1988).

Early cleavage division in mouse embryos appears to conform to the model of the adult cell cycle, at least superficially. After fertilization, the cell goes through G_1 and S phases, a short G_2 and M, over the course of 17 to 20 hours (Howlett and Bolton, 1985; Howlett, 1986; Luthardt and Donahue, 1975). Subsequently, the cells divide every 10 to 14 hours and appear to express G_1, S and G_2 phases in the cell cycles following the first mitosis (Bolton et al., 1984; Sawicki et al., 1978), and growth and proliferation are responsive to growth factors (Rappolee et al., 1992). Considerably later in development (rat d.g. (days of gestation) 10, mouse d.g. 9), analysis of the cell cycle in the neuroepithelium revealed a cell cycle time of approximately 9 hours (Kauffman, 1968; Mirkes et al., 1989). The cells express a G_1 phase of approximately 2 hours, and S and G_2 are similar to those seen in most normal, rapidly proliferating adult cells.

Very little is known about the cell cycle during the 5 days of development in rodents that separate implantation and the onset of neurulation. Growth rate, and presumably cell cycle structure, are not constant through this period of development, but respond to both environmental and developmental cues (Lewis and Rossant, 1982). The onset of gastrulation in mice has been associated with a dramatic increase in growth rate and shortening of the cell cycle within the embryo. Several studies have provided an estimate of 7 to 7.5 hours for cell cycle length during gastrulation (Lawson et al., 1991; Poelmann, 1981; Snow, 1977; Solter et al., 1971). One study (Snow, 1977) also suggested that there is a population of cells, termed the proliferative zone (PZ), at the anterior end of the primitive streak, in the region analogous to Hensen's node, that has a cell cycle time of approximately 3 hours. The other studies failed to find evidence for this population, but did not address the question directly.

It is clear that the cell cycle structure is regulated directly during mammalian embryogenesis and that these changes are an integral part of development. The radical abbreviations of the cell cycle during gastrulation would appear to require shortening of phases of the cell cycle other than G_1, distinguishing growth regulation during this developmental period from that found in mature cells. It would appear that the rodent embryo has the capacity to override some cell cycle checkpoints during development. Since regulation of growth is an integral part of development, we felt clarification of the cell cycle structure during gastrulation was an essential step toward understanding how the cell cycle is regulated during embryonic development. The questions addressed in this paper are, first, whether there are subpopulations of cells within the embryo that are characterized by different cell cycle times and, second, what are the lengths and structures of the cell cycles in the embryo during gastrulation.

MATERIALS AND METHODS

Embryo culture

Embryos were explanted from time-mated Sprague-Dawley rats (Tyler Labs, Bellevue, WA) starting at 1:00 p.m. on d.g. 8 (day of vaginal plug = day 0) by standard techniques and were in culture by 3:00 to 4:00 p.m. (Fujinaga and Baden, 1991). Briefly, the implantation sites were removed from the uterus and opened to reveal the embryo. Reichert's membrane was removed and the embryos placed in culture medium. Culture medium was composed of 80% rat serum, collected from the animals at the time of killing, and 20% Hanks' buffered saline (HBSS), all equilibrated with a gas mixture of 90% N_2, 5% O_2, and 5% CO_2. The embryos were then incubated at 37°C with rolling. Use of this method has been shown to support growth that parallels development in vivo for up to 48 to 72 hours of culture (Fujinaga and Baden, 1991). After explantation the embryos were cultured for 3.5 to 4 hours to allow them to recover and begin growing again before experiments were started between 7:00 and 8:00 p.m. on d.g. 8.

Nocodazole treatment of embryos in culture

Much of the work was based on a stathmokinetic analysis of the cell cycle in which nocodazole (Sigma) was used to block passage through mitosis; nocodazole destabilizes microtubules and prevents passage through mitosis. Nocodazole in dimethyl sulphoxide (DMSO) at 0.4 mg ml^{-1} was added to a final concentration of 0.4 μg ml^{-1}. Addition of the same volume of DMSO alone to embryos in culture had no discernible effect on the distribution of cells through the cell cycle as revealed by flow cytometry (FCM). Addition of nocodazole to 0.04 μg ml^{-1} did not give as rapid or complete an arrest as 0.4 μg ml^{-1} final, while increasing the nocodazole concentration to 1.2 μg ml^{-1} did not enhance the rate of arrest. Nocodazole was used at 0.4 μg ml^{-1} in all subsequent experiments. Release from nocodazole was rapid and fairly uniform following transfer of the embryo to nocodazole-free medium. In preliminary experiments, embryos treated with nocodazole for 6 hours were moved to nocodazole-free medium and samples were taken every 10 minutes for 90 minutes. The embryos were fixed in 4% formaldehyde overnight, washed and

then permeabilized by treating with 0.1% NP-40 in phosphate-buffered saline (PBS). The DNA was stained with 4,6-diamidino-2-phenylindole (DAPI) in water (10 μg ml^{-1}) and the embryos examined in whole mount by fluorescence. Within 30 minutes of transfer to nocodazole-free medium, the majority of cells had entered metaphase and by 50 minutes after release from the mitotic block essentially all cells were in anaphase or telophase. For experiments in which the number of cells arrested in mitosis during nocodazole treatment was to be determined by histological examination, the embryos were transferred from the medium containing nocodazole to nocodazole-free medium for 30 minutes to allow the arrested cells to enter metaphase and anaphase, as these phases of mitosis could be scored easily. For experiments in which the embryos were to be examined by FCM, the embryos were removed from culture and the ectoplacental cone and much of the adjacent extraembryonic tissue were removed and discarded, the embryos washed once each in cold HBSS and PBS, placed in PBS with 10% DMSO and frozen at −20°C.

Histological preparation of embryos

Embryos were removed from culture and washed once each in cold HBSS and PBS, and then fixed overnight at 4°C in 2% glutaraldehyde (Sigma) in 0.15 M sodium phosphate (pH 7.4). After fixation, the embryos were washed several times with PBS, dehydrated through an ethanol series and embedded in a methacrylate resin (Polaron, BioRad). All sections were cut at 3 μm. Because examination of the sections showed that most cells were 8 to 10 μm or smaller, counts were collected from every fourth section to yield nonoverlapping data. To determine the mitotic index, sections were stained with toluidine blue (1% in water), which gives strong staining of basement membrane in addition to condensed chromosomes and background staining of the rest of the cell. Staining of the basement membrane made it easier to distinguish the ectoderm, which expresses basement membrane, from the primitive streak, which does not. Only cells in which some portion of the nucleus was clearly visible in the section were counted.

[^{3}H]thymidine labelling and autoradiography

To ensure exposure of the ectoderm and mesoderm to [^{3}H]thymidine, we removed the ectoplacental cone at the time [^{3}H]thymidine was added to the culture, so that the proamniotic cavity was exposed to the medium. The manipulations were performed in prewarmed medium and on batches of 5 to 10 embryos to minimize the time out of culture and consequent perturbations of the cell cycle. [^{3}H]thymidine (Amersham, 925 Gbq $mmol^{-1}$) was added to 5 μCi ml^{-1} final concentration and the embryos returned to culture at 37°C. After culture the embryos were fixed, embedded and sectioned as described above. As preparation for autoradiography, the sections were washed thoroughly with water and then dipped in emulsion (NTB-2, Eastman-Kodak) and exposed at 4°C for two days to two weeks as required. The autoradiographs were developed in Dektol (Kodak) and fixed, counterstained with toluidine blue, dehydrated and covered with a coverslip. Cells were considered to be positive for [^{3}H]thymidine incorporation if they had three or more grains over the nucleus.

Flow cytometry

Samples, composed of two to four embryos, were thawed on ice and the PBS/DMSO mixture removed. The embryos were resuspended by gentle agitation with 0.1% NP-40 in 147 mM NaCl, 10 mM Tris-HCl pH 7.4, 2 mM $CaCl_2$, and 22 mM $MgCl_2$ with 10 μg ml^{-1} DAPI to provide a nuclear suspension and analyzed by FCM with a Phywe ICP-22 flow cytometer interfaced with a PDP 11/23 computer (Digital Equipment Co.). The data were analyzed using the Multicycle program (Phoenix Flow System, San Diego, CA).

Cell volume measurements

Cell volumes were estimated by measuring the dimensions of cells perpendicular and parallel to the plane of the ectoderm. The dimensions were derived from photomicrographs and the scale determined from a photomicrograph at the same magnification of a 100 μm standard. The cells of the ectoderm were assumed to be cylindrical for the volume calculations, a reasonable assumption based on examination of the different planes of section through the embryos. The cells of the PS were assumed to be prolate spheroids in which the axis of rotation was perpendicular to the plane of the ectodermal tissue.

RESULTS

Very rapid proliferation of cells in the primitive streak

As a first step toward understanding growth regulation during early rodent development, we chose to address the question of cell cycle length during gastrulation. The increase in mitotic index over time during mitotic arrest by nocodazole was used to determine whether there were any identifiable populations of cells that cycled at different rates. We used an embryo culture system that has been shown to support growth of rat embryos explanted at the time of gastrulation that essentially parallels growth in vivo for up to 72 hours (Fujinaga and Baden, 1991). Growing embryos in vitro allowed a more controlled and reproducible manipulation of the embryo.

The embryo was subdivided into three regions for analysis: the ectoderm without the primitive streak (Fig. 1B,D); the primitive streak, defined for the purposes of this report as only the specialized region of the ectoderm indicated and not including any cells that had delaminated from the ectoderm (Fig. 1B,D); and the mesoderm, all cells that had delaminated from the ectoderm, including cells immediately underlying the PS (Fig. 1B,D). The primitive streak (PS) of an embryo cultured in vitro but not exposed to nocodazole is shown in Fig. 1E. The cells of the PS are characterized by a smaller size and more rounded appearance than the cells of the ectoderm. The volume of cells in the PS was estimated to be 37±20% that of the cells in the ectoderm (50 cells for each population collected from a total of 10 sections from 4 embryos; $P<0.01$ by paired t-test) as described in Materials and Methods. The lack of a well-organized basement membrane under the PS is reflected in the relatively poor toluidine blue staining of the membrane of the cells in the PS compared with that of the cells of the ectoderm. The endoderm was not included in this analysis, in part because the cells at this stage are largely extraembryonic. Further, a good estimate of its cell cycle length (10 to 11 hours) already exists (Lawson et al., 1987).

The percentage of cells in mitosis as a function of time in the presence of nocodazole are plotted in Fig. 2. The most important point that can be derived from these results is that the cells of the PS arrested significantly more rapidly than the cells of the ectoderm or the mesoderm. The PS was unique in that it was the only identifiable subpopulation within the embryo that emerged from this analysis as having a significantly different cell cycle time. The estimated lengths of the cell cycles, derived by extrapolation

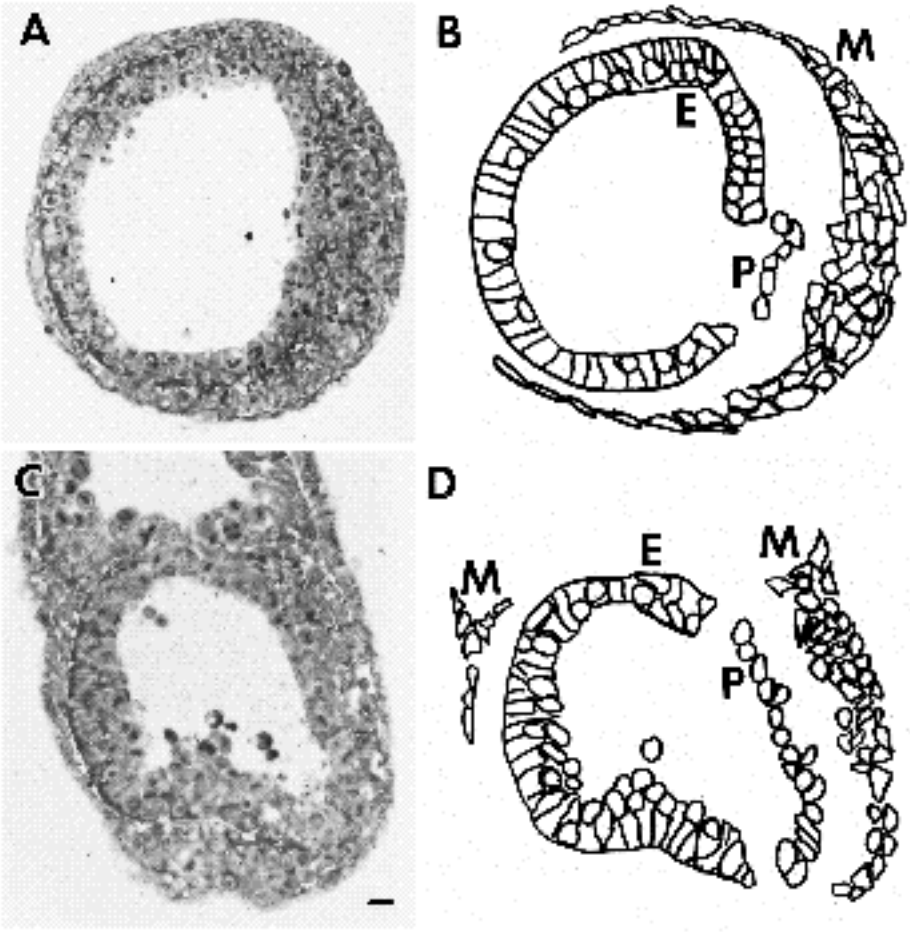

Fig. 1. Representative sections of embryos treated with nocodazole. Rat embryos explanted on d.g. 8.5 and grown in culture were incubated in nocodazole for 3 hours. The embryos were cultured in nocodazole-free medium for 30 minutes, and prepared for analysis as described in Materials and Methods. Representative sections are shown in cross section (A) or longitudinal section (C). Bars indicate 10 μm. The cartoons were traced from the photomicrographs, with the populations separated to indicate the subdivisions of the embryo used for determining mitotic indices: (B) cross section, (D) longitudinal section. In panels B and D, E is the ectoderm, the columnar epithelium of the innermost layer of cells; P is the primitive streak; and M is the mesoderm, the relatively dispersed mesenchymal cells that separate the ectoderm and endoderm. The outermost layer of cells is the primitive endoderm (not shown). (E) Cross section of an embryo not treated with nocodazole (detail of the PS). The edges of the PS are marked by arrowheads. (F) Scheme of a rat embryo during gastrulation (d.g. 8.5) showing the relative positions of the cell populations in the embryo.

of the mitotic index to 100%, were 3 to 4 hours for the PS and 7 to 8 hours for the mesodermal and ectodermal cells. The cells of the mesoderm immediately underlying the PS were also examined as a separate population. We thought that the extreme rapidity of cell division in the PS might have an effect on the cell cycle of these cells relative to the other cells of the mesoderm. There was no significant difference in the rate of mitotic arrest between the mesoderm of the PS and the mesoderm as a whole (paired *t*-test, $P>0.25$), suggesting similar growth rates for these two populations (data not shown). Although the mesoderm of the PS appears to be an homogeneous population, the scatter

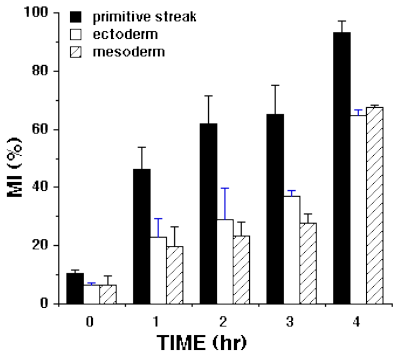

Fig. 2. Time course of mitotic arrest induced by nocodazole. The mitotic indices were determined for each of the three populations indicated in Fig. 1. Five to seven sections from each of three to four embryos at each time point were collected from three experiments, counted and averaged. The mitotic index (MI) is expressed as the percentage of cells in mitosis in a given population and plotted against the time of incubation in nocodazole. Nocodazole was added to the culture at zero hour and samples removed to nocodazole-free medium at hourly intervals, incubated for 30 minutes and then processed for histology. The MI of the PS differs significantly from that of the ectoderm and mesoderm (paired *t*-test, $P<0.05$) at all times. Bars indicate s.d.

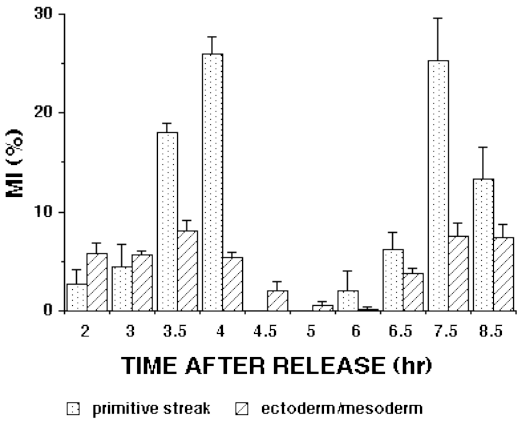

Fig. 3. Determination of cell cycle length in embryos partially synchronized by mitotic arrest. Explanted rat embryos were cultured in the presence of nocodazole for 90 minutes and then moved to nocodazole-free medium at zero hour. Embryos were removed after various times of culture in nocodazole-free medium and the mitotic indices (MI) determined for ectoderm, PS and mesoderm as described in Materials and Methods. Each point represents the average for four to six sections from each of three to six embryos. The data were collected from two different experiments with embryos from five litters. The mitotic index was plotted against the length of time the embryos had been in nocodazole-free medium. Bars indicate s.d.

in the data would have prevented detection of small inhomogeneities.

Previous work had identified only the cells at the anterior end of the PS as having a 3-hour cell cycle time (Snow, 1977). To facilitate analysis of the cells around and in the anterior end of the PS, embryos were examined in both longitudinal and cross sections. Several of the longitudinal sections displayed the PS along the anterior-posterior axis (Fig. 1C,D). After three hours in nocodazole, most of the cells (75 to 80%) along the length of the PS had been arrested in mitosis or were in late G_2, showing no evidence of variation in the rate of arrest with position in the PS. In this and subsequent experiments, there was no detectable difference in cell cycle time between anterior and posterior ends of the PS. It was also clear from this analysis that cells of the ectoderm immediately anterior to the PS were similar in their rate of arrest to the ectoderm as a whole rather than to the PS. From this, we concluded that the cells lying immediately anterior to the PS were not cycling significantly more rapidly than other ectodermal cells.

Determination of cell cycle durations

To generate a more accurate estimate of the length of the two different cell cycles in the embryo, we determined the time between consecutive mitoses. The embryos were treated with nocodazole for 90 minutes to enrich for cells in mitosis. The nocodazole was removed and the cells allowed to resume cycling. After release from nocodazole arrest, the cells should enter mitosis and proceed through the next cell cycle synchronously. The mitotic index should drop during the phase of the cell cycle depleted by nocodazole arrest and then rise again, peaking as the synchronized cells enter the next mitosis, approximately 1 cell cycle length after removal of nocodazole.

Mitotic indices were determined at the times indicated for the same populations described above: ectoderm, mesoderm and PS. Two well-defined peaks in the mitotic index were seen for the PS. The first occurred between 3.5 and 4 hours and the second at approximately 7.5 hours (Fig. 3). The cell cycle time interpolated from these data was 3 to 3.5 hours, in agreement with the time derived by nocodazole arrest. A similar plot of the mitotic index for ectoderm/mesoderm showed the expected pattern, with a peak at 7.5 to 8.5 hours after nocodazole release (Fig. 3). After subtracting 30 to 45 minutes as the time required for recovery from nocodazole arrest, the estimated cell cycle time is 7 to 7.5 hours. The period of nocodazole arrest represents 20% of the cell cycle for cells of the ectoderm and mesoderm (90 minutes of 450 minutes) but 50% of the cycle for cells in the PS (90 minutes of 180 minutes); therefore, a smaller percentage of cells would have been arrested in the ectoderm and mesoderm than in the PS (approximately 20% and 50% arrested, respectively), resulting in a less pronounced peak in the mitotic index for the ectoderm and mesoderm than for the PS.

Determination of the lengths of G_1 and S

Analysis of the mitotic index provided estimates of cell cycle lengths and their distribution in the embryo but no information about the structure of the cell cycle. Simple deletion of G_1 from any of the adult cell cycles described previously ($S+G_2+M=9$ to 12 hours) would not shorten the cell division time sufficiently to account for even the longer cell cycle of the ectoderm and mesoderm. The distribution of cells between G_1, S and G_2/M can be derived from an analysis of the DNA content of cells in the embryo by FCM. The lengths of G_1 and S were derived by determining the time required to deplete these phases of the cell cycle during

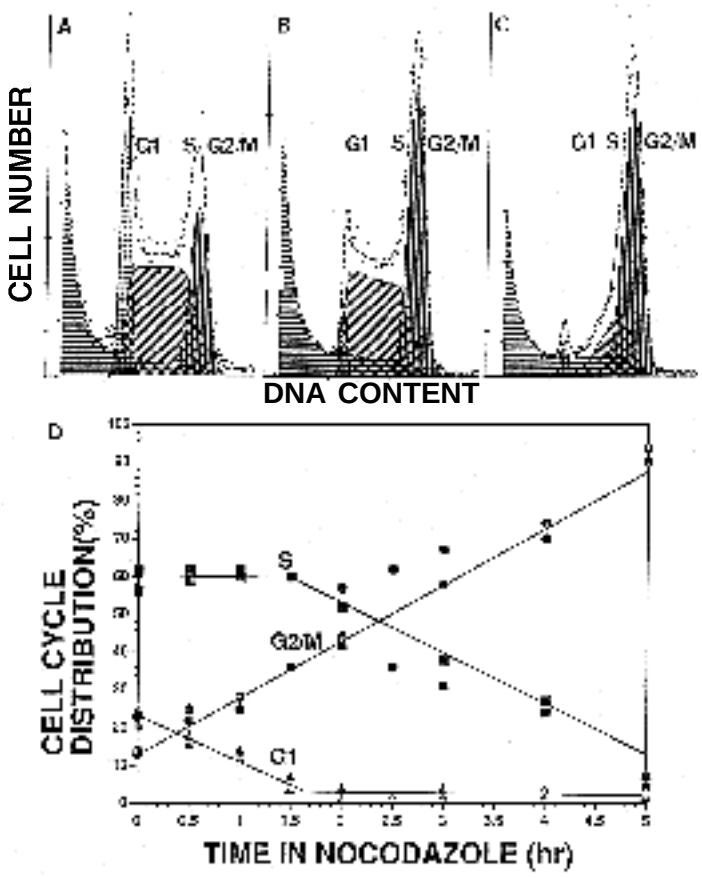

Fig. 4. Analysis of the cell cycle by FCM during nocodazole arrest. For each experiment, eight litters were explanted into culture, nocodazole was added at zero hour and 10 embryos were removed at each of the times indicated and prepared for FCM as described. The nuclear suspensions were analyzed by FCM, which gives DNA content per nucleus or nuclear fragment. The raw data are shown in panels A, B and C as crosses and the dashed line represents the smoothed curve. The data are plotted as relative fluorescence (x-axis) against the number of events (y-axis). The population was subdivided to give estimates of the relative sizes of the G_1 (speckled fill), S (diagonal lines) and G_2/M (vertical lines) populations. The curve starting at the far left of the plot and indicated by the horizontal crosshatching is composed of nuclear fragments and cellular debris. Results of FCM analysis of a single experiment are shown for a control population, not treated with nocodazole (A); embryos cultured in nocodazole for two hours (B); and embryos cultured in nocodazole for four hours (C). Plots such as those shown in panels A, B and C were also used to give estimates of the percentage of cells in G_1, S and G_2/M. The results from the two most complete FCM analyses (of four) are combined and plotted in panel D. Percentage of cells in G_1 (triangles), S (squares), and G_2/M (circles) are shown.

nocodazole arrest. G_1 would start to decline immediately after the addition of nocodazole. When G_1 is depleted and no further cells could enter S, then S would start to decline. The length of S is measured from the time the last cells entered S to the time it is depleted. The cells of the ectoderm and mesoderm constitute the majority of the embryo and are the only cells expected to contribute significantly to the FCM analysis. The PS and endoderm represent relatively small fractions of the total (2% to 5%, and 10% to 15%, respectively) and would have little impact on this analysis.

Representative plots from the FCM analysis are shown in Fig. 4A-C. Embryos not exposed to nocodazole showed approximately 25% of the cells in G_1, 60% of the cells in S phase and the remainder in G_2/M (Fig. 4A). These estimates of the distribution of cells through the cell cycle are consistent with rapid proliferation and the active involvement of most cells in growth. Within two hours of the addition of nocodazole, the percentage of cells in G_1 had dropped to 0.5%, with a corresponding increase in cells in G_2/M (Fig. 4B). After three hours in the presence of nocodazole, the percentage of cells in S had started to decline (Fig. 4C). The accumulation of debris during the nocodazole arrest was presumed to result from the disintegration of cells arrested in mitosis for an extended period of time, as has been suggested in other systems (Kung et al., 1990).

The results from the FCM analysis are plotted in Fig. 4D, which shows the percentage of nuclei with G_1, S or G_2/M DNA content at various times during the nocodazole arrest. The fraction of cells in G_1 decreased to a plateau of 1% to 3% within 1.5 to 2 hours of the addition of nocodazole. From these data, we estimated the length of G_1 to be 1.5 to 2 hours for most cells in the embryo. The ability to deplete the G_1 population almost completely during nocodazole arrest indicated that essentially all cells in the embryo were cycling actively. The fraction of cells in G_1 showed a linear decrease during nocodazole arrest, suggesting that G_1 was the same length for most cells in the embryo and that passage of cells through the cell cycle was not slowed by incubation in nocodazole. The apparent lack of an inhibitory effect of nocodazole on passage through the cell cycle provided greater confidence in the estimates of cell cycle length derived as described above.

The residual 1 to 3% of cells that remained in G_1 after nocodazole treatment may represent: (1) cells that had escaped the nocodazole block, but were unable to continue cycling, would have appeared in G_1 briefly before decaying into subcellular debris; (2) endodermal cells have a 10- to 11-hour cycle time and, if the difference in division time is largely a result of change in the length of G_1, could contribute to this population; (3) a small population of noncycling, G_0, cells or cells that were cycling very slowly.

Depletion of S started between 1.5 and 2 hours when cells stopped entering S from G_1. Extrapolation of the line for the fraction of cells in S to zero yielded an estimate of approximately 4 hours for the length of S (Fig. 4D). There was no evidence for any substantial subpopulations that expressed detectably different cell cycle times, although a population of up to 20% of the cells of the embryo would have been hard to detect. The earlier time points were considered more reliable in determination of the line for several reasons. The condensed chromosomes of late prophase bind less DAPI than do more extended chromosomes. Continued condensation of the chromosomes with extended nocodazole arrest resulted in the appearance of nuclei that appeared to contain less than a G_2/M DNA content, and confused the assignment of nuclei to S phase versus G_2/M. The rapid accumulation of cellular debris at the later time points provided a background that changed over time and complicated interpretation of the data. The number of cells

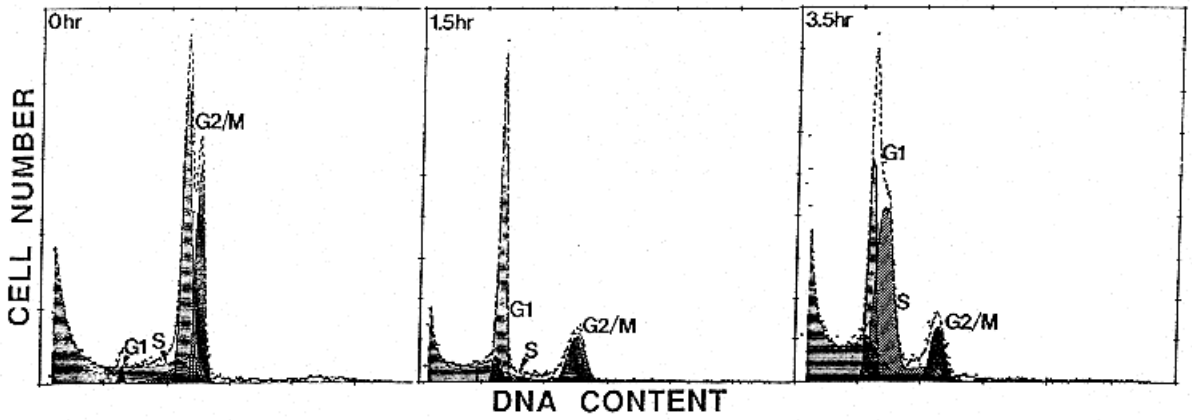

Fig. 5. Cell cycle progression in embryos synchronized by mitotic arrest. Embryos were cultured in nocodazole for six hours, at which point approximately 85% of the cells in the embryo should be in G_2/M. The embryos were washed, cultured in nocodazole-free medium and cell cycle distribution determined by FCM analysis of DNA content at the time the embryos were moved to nocodazole-free medium (zero hour), and at 1.5 hours and 3.5 hours after removal of nocodazole. The plots shown are from one of three, and represent 10 embryos at each time point drawn at random from 10 litters. The positions of the G_1 (speckled fill), S (diagonal lines) and G_2/M (vertical lines) populations are indicated on the panels. The curve starting at the far left of each panel and indicated by the horizontal lines is composed of nuclear fragments and cellular debris.

lost as debris did not appear to have a profound effect on the interpretation of the data, particularly at the early time points, and so was ignored for simplicity.

Release from mitotic arrest reveals a rapidly cycling 'G_1-less' population

As an alternative approach to determining the lengths of G_1 and S, FCM was used to follow a synchronized population of cells through a cell cycle. Monitoring the time at which cells began to enter S and then G_2/M gave estimates of the lengths of G_1 and S, respectively. A six hour nocodazole treatment was used to arrest the cells and, after release from nocodazole, the progress of the synchronized cells through the next cell cycle was analyzed. The estimates of the lengths of G_1 and S from this analysis were the same as those derived from analysis of the nocodazole arrest. The FCM analysis at 1.5 hours provided evidence for a small population of cells (less than 5% of the cells of the embryo) that had already entered S (compare 0 and 1.5 hours in Fig. 5). These cells were in late S 3.5 hours after release from nocodazole arrest, consistent with a cell cycle time of approximately 3.5 hours (Fig. 5). This latter population probably represents the cells of the PS, although this is not certain. The rapidity with which these cells entered S provides indirect evidence that G_1 is very short for the cells of the PS, probably less than 30 minutes.

Determination of the length of G_2

FCM analysis does not distinguish G_2 from M and so did not provide any information about the duration of G_2. The length of G_2 was estimated by determining the time between the addition of [^{3}H]thymidine and the appearance of radiolabelled mitotic figures. As shown in Fig. 6A and summarized in Table 1, mitotic figures in the PS judged as being in late prophase were labelled within 30 minutes of the addition of [^{3}H]thymidine, and mitotic figures in the mesoderm and ectoderm were labelled by 50 minutes (Fig. 6B). After a 70 minute incubation, all phases of mitosis in the PS and metaphase figures in the ectoderm were labelled (Fig. 6C). Using an estimate of 10 to 20 minutes from the onset of mitosis to the point at which a cell could be detected as being in late prophase, we estimated G_2 as less than 20 minutes for the cells of the PS and 30 to 40 minutes for the mesodermal and ectodermal cells. The slowing of the rate of DNA synthesis that occurs toward the end of S renders a precise mapping of its end difficult and tends to give an overestimate of the length of G_2; thus, G_2 in the cells of the PS was probably substantially less than the estimated 20 minutes and may have been essentially nonexistent. Similarly, G_2 in the mesodermal and ectodermal cells was probably significantly shorter than the estimated 30 to 40 minutes.

Table 1. Appearance of [^{3}H]thymidine-labelled mitotic figures

Tissue layer	Time of appearance, minutes			
	30	50	70	90
Primitive streak	P	M	All	
Ectoderm and Mesoderm	−	P	M	All

The data derived from the experiment shown in Fig. 6 are summarized in this Table. The sample times are expressed as minutes from the time of addition of [^{3}H]thymidine to the cultured embryos. Four to six sections from each of six embryos were examined at each time point. The appearance of grains over mitotic figures is indicated by identifying the latest phase in mitosis labelled within either the PS or the ectoderm and mesoderm. P= late prophase, prometaphase; M= metaphase; All= all phases of mitosis are labelled.

Determination of labelling index

As an independent approach to assess the validity of the cell cycle information derived by nocodazole arrest, the fraction of cells in S phase was estimated from the labelling index. After a 10 minute incubation in [^{3}H]thymidine, four

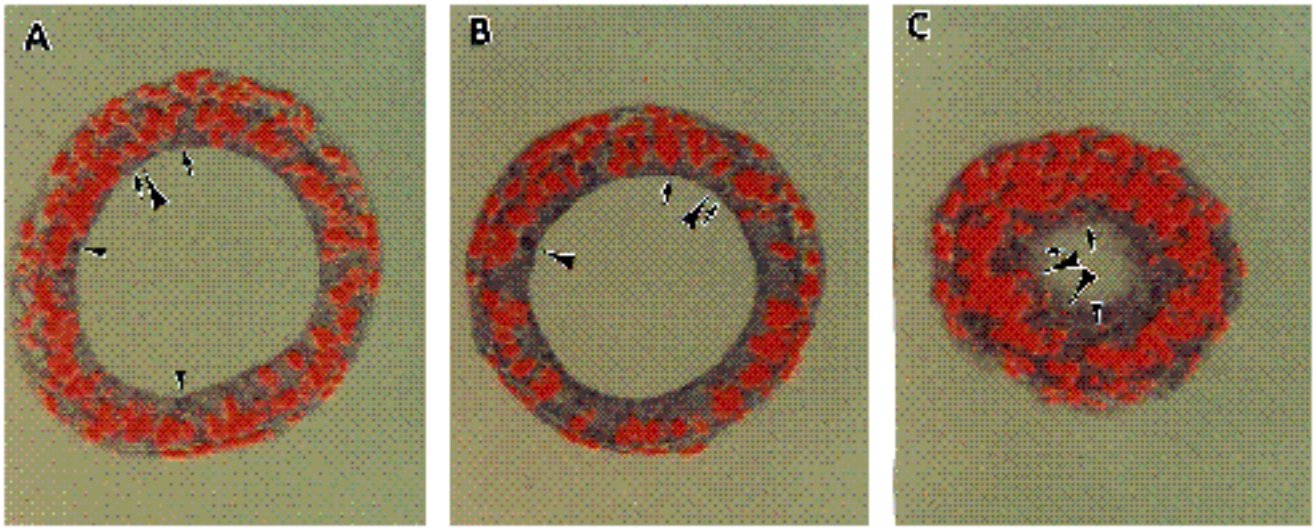

Fig. 6. Determination of the length of G_2. Embryos that had been incubated in the presence of [^{3}H]thymidine for 30 minutes (A), 50 minutes (B), or 70 minutes (C) were prepared as described in Materials and Methods. The sections were autoradiographed for 5 days (A), 3 days (B) or 2 days (C). The slides were counterstained with toluidine blue to show the mitotic figures. Labelled mitoses are indicated by large arrowheads, and unlabelled mitoses by small arrowheads. The limits of the PS are indicated by arrows. Bar indicates 5 μm.

to six sections were analyzed from each of six embryos. The labelling indices of the mesodermal and ectodermal cells were 61±4% and 65±6%, respectively, in good agreement with the percentage of cells in S phase estimated by FCM, approximately 62%. The labelling index in the PS appeared to be slightly higher, 73±5%, which was significantly different from that of the ectoderm and mesoderm by paired *t*-test ($P<0.05$). This measure of the fraction of PS cells in S phase corresponds with estimates based on cell cycle information derived above. The estimates of the proportion of cells in S for each of these populations derived from the labelling index are very close to the estimates derived from the data presented above, suggesting that the presence of nocodazole resulted in neither an artefactual increase in the rate of proliferation in the PS, nor slowed the ectoderm or mesoderm. The consistency of the interpretations from several different types of analysis provide internal confirmation for the results reported here. The results of the cell cycle analyses are summarized in Table 2.

Table 2. Summary of cell cycle data for d.g. 8.5 rat embryos

Tissue layer	G_1	S	G_2	M*
Ectoderm	1.5-2 hr	3.5-4 hr	<40 min	0.75 hr
Primitive streak	<0.5 hr	2-2.75 hr	<20 min	0.75 hr
Mesoderm	1.5-2 hr	3.5-4 hr	<40 min	0.75 hr

The estimates of the lengths of the phases of the cell cycle derived from the experiments described are presented. The times for G_1 and S are derived from the FCM analyses and are stated as ranges that we feel reflect the variation in length of these phases within the population. G_2 was derived from the appearance of the first labelled mitotic figures within a population.

*Mitosis was assumed to be 0.75 hours.

DISCUSSION

We have shown that dramatic alterations in cell cycle length and structure occur as developmental decisions are made during gastrulation in rat embryos. The changes in cell cycle structure suggest that proliferation is regulated differently during gastrulation than at any other stage of development. The cells of the mesoderm and ectoderm outside the PS have a cell cycle time of 7 to 7.5 hours, whereas cells within the PS have a cycle time of 3 to 3.5 hours. These rates of cell division are in accord with previous estimates for this developmental stage (Lawson et al., 1991; Poelmann, 1981; Snow, 1977; Solter et al., 1971); however, we have also described the cell cycle structures and have redefined the nature of the highly proliferative zone of cells within the embryo.

The structures of the cell cycles showed several unexpected features. The cell cycle during gastrulation was shortened by substantially reducing the lengths of S and G_2, in contrast to the adult cell cycle, in which they are relatively constant and G_1 is variable. The cell cycle expressed in the ectodermal and mesodermal cells appeared to have a G_1 of 1.5 to 2 hours, similar in length to the G_1 seen in rapidly growing adult cells such as those of the intestinal crypt (Loeffler et al., 1986). The cells of the ectoderm and mesoderm appeared to act as homogeneous populations, but if a relatively small population of cells (20% or less of the total) was distributed throughout the embryo, it would have been hard to detect in this analysis. The cells of the PS were more radical in that they appeared to have shortened G_1, S and G_2 further, perhaps to the point of effectively eliminating G_1 and G_2. The estimates of G_1 and G_2 that we derived, less than 30 and 20 minutes, respectively, are likely to be overestimates. The length of G_1 in the PS is based

on two lines of indirect evidence, the FCM data and the labelling index. The conclusion from both experiments was that there is a population of cells in which G_1 is very short and that these cells are in the PS. The cell cycle in the PS seems to approximate a simple S/M cycle. We believe that most, if not all, cells that cross the PS have undergone at least one rapid cell cycle based on the significant reduction in cell volume for most cells in the PS (see Discussion below).

Identification of a highly proliferative zone

We derived evidence for a region of cells of high proliferative activity as has been described previously (Snow, 1977), but we have redefined the nature of the proliferative zone (PZ) on two levels: first, its location, and second, that it is a transient rather than a stem cell population. The region of highest proliferative activity appears to include the whole PS, but is limited only to cells within the PS and does not include the ectodermal cells that surround the anterior end of the PS. Originally, the anterior end of the PS, the structural homologue of Hensen's node, had been identified as the PZ (Snow, 1977). This conclusion was based on the mitotic index in undisturbed embryos, a form of analysis that is very sensitive to even small changes in cell size and orientation within the section. We chose to manipulate the cell cycle directly using several complementary methods involving perturbation and labelling, so that problems resulting from potential bias or lack of sensitivity inherent in the other approaches were reduced. It is possible that the nature of the PZ differs between mice and rats, but the similar patterns of growth and development of the two species suggest that this is unlikely.

Does cell cycle regulation reflect aspects of developmental regulation during gastrulation?

Two fundamental developmental decisions in rat embryos are marked by changes in the cell cycle. First, all the cells that contribute to the mesoderm and endoderm migrate through the PS. Cells in the ectoderm divide approximately every 7 hours. As cells enter the PS, leaving the ectoderm proper, they shorten G_1, S and G_2 phases of the cell cycle and begin to divide with a 3- to 3.5-hour cell cycle. The rate of cell division appears to slow as soon as the cells exit the PS and become part of the mesoderm. It has been demonstrated with great elegance that the cells of the PS are a transient population (Lawson et al., 1991), and so the growth kinetics of the cells that traverse the PS would not appear as profoundly different from cells that remain in the ectoderm as would be expected if the PS were a stem cell population. Examination of the cell growth data from Lawson et al. (1991) reveals a greater than expected number of cells that gave rise to disproportionately large numbers of descendants, consistent with some of the cells having divided more rapidly than expected, at least for a brief period. Regional variations in the cell cycle reflect elements of the emerging body plan, specifically the anterior/posterior axis and germ layer formation.

Second, the onset of gastrulation is associated with an increased rate of growth and proliferation in the embryo as a whole. We do not know if growth changes abruptly with the onset of gastrulation or if the change is gradual, but previous work suggests that a cell cycle time of 10 to 12 hours is maintained at least until the final 6 to 12 hours before gastrulation (Snow, 1977). Because of the nature of the experiments, a wide range of developmental ages were examined (from within a few hours of the onset of gastrulation, at approximately noon of d.g. 8 through early d.g. 9) and it seems that the structures of the cell cycle that we have reported are maintained throughout gastrulation. The transition from the rapid cell cycles found during gastrulation to the adult form appears to be achieved in a series of steps by first lengthening S and G_2 to resemble the rapid cell cycles seen in adult tissues, before G_1 shows significant changes (Kauffman, 1968; Mirkes et al., 1989). It seems likely that the process is considerably more complex than has been suggested so far and is tightly linked with the process of development.

Cell cycle regulation during gastrulation: G_1 checkpoints

The requirement for increases in both mass and cell number in the early mouse embryo limits the possible cell cycle structures that could be used in ways that do not limit the early proliferation of *Xenopus* and *Drosophila*. The smaller size of the cells of the PS presumably results from their extremely rapid proliferation. We were unable to derive direct estimates for the length of G_1 or S in the PS, but indirect evidence suggests that G_1 is less than 30 minutes and may be considerably shorter. It is possible that these cells lack any significant G_1 phase and that growth and proliferation are uncoupled in the PS, at least in part. Regulation of passage through G_1 is the usual mode that cells use to link cell growth and division, and cell size is reduced in yeast mutants that lack normal G_1 control (reviewed in Cross et al., 1989). Cells of the PS appear to act as an homogenous but distinct population in that all parameters of the cell cycle appear to be more rapid than in the ectoderm and mesoderm. The appearance of the two peaks in the MI in the PS (Fig. 3) also supports this interpretation and renders unlikely the possibility that cells enter the PS at a specific point in the cell cycle as synchrony in the population would be lost very rapidly in this case.

Mesodermal and ectodermal cells express a G_1 phase of about 2 hours, similar in length to that seen in some rapidly growing adult cells. G_1 phases of this length are obviously compatible with normal size regulation in the early embryo, and may be required to ensure that growth and proliferation remain linked despite the rapid rate of cell division, although other explanations are possible. The presence of G_1 suggests that these cells do express some form of G_1 regulation, but its brevity may require modification of aspects of the regulation, such as growth factor dependence. Fibroblast growth factor-4 is expressed within the anterior part of the PS and in the ectoderm and mesoderm immediately adjacent to it, suggesting that it does not drive the rapid proliferation seen in the PS itself (Niswander and Martin, 1992). As yet no molecules have been described that have a pattern of expression that coincides with the rapidly proliferating cells in the PS, leaving us with no indication as to how the change in cell cycle regulation is effected.

Regulation of entry into S is presumably equivalent to

regulation of G_1. In the adult cell cycle, passage through S is largely independent of external conditions and relatively invariant in length. Two different mechanisms may be used to accomplish the shortening of S phase. First, the time over which replicons are initiated may be compressed so that the time between the firing of the first and last replicons is reduced. Second, a greater number of replicons may be used. These two possibilities are not exclusive; both are used in the early, rapid cleavages of *Drosophila* to allow rapid replication of DNA (Blumenthal et al., 1974; McKnight and Miller, 1977).

Cell cycle regulation during gastrulation: G_2 checkpoints

The shortening of G_2 in the mammalian embryo during gastrulation, and its possible elimination from the cells of the PS, distinguishes these embryonic cells from normal adult mammalian cells, in which the length of G_2 is relatively invariant at 1.5 to 2 hours. One important question that arises is whether some of the regulatory functions normally expressed in G_2 are modified or eliminated during this period of rapid growth, and whether there are any consequences for the embryo. In *Drosophila* and *Xenopus* cell cycles that lack detectable G_2 phases, the ability of the cells to arrest cell cycle progression in response to incomplete DNA synthesis or DNA damage is substantially modified or abrogated (Dasso and Newport, 1990; Kimelman et al., 1987; Raff and Glover, 1988). It might be expected that agents that induce G_2 arrest in more mature cells - radiation, DNA alkylation, incomplete DNA synthesis - would fail to do so in the PS, and perhaps in all cells in the rodent embryo during gastrulation, impairing the ability of the cells to effect repair and thus enhancing the toxicity of these agents. The exquisite sensitivity of rodent embryos in vivo to damage by these agents during gastrulation relative to other stages of development suggests that some aspects of G_2 regulation are altered. Whether a loss of G_2 regulation is involved in this greater sensitivity is not clear from the in vivo experiments, but is being addressed in vitro.

Why such rapid proliferation and what does it cost?

Regulation of the cell cycle during rodent embryogenesis stands in contrast to its regulation during *Drosophila* and *Xenopus* development. Mammalian embryos start gastrulation with relatively few cells (200 to 300 cells per embryo for mice) (Snow, 1977). One of the goals of gastrulation may be the generation of enough cells to provide a template with the positional information typical of an embryo by the end of gastrulation. Based on information derived from other systems, it seems likely that the potential costs to the embryo of very rapid proliferation would be high in terms of the production of damaged cells (Hartwell and Smith, 1985; Minden et al., 1989; Sullivan et al., 1990). The potential costs must be balanced by the developmental role that is played by the rapid growth during gastrulation. One possibility is that the adaptations that allow growth while cells migrate through the PS have as a consequence the loss of G_1 and G_2. An alternative explanation that implies a more direct purpose for the increased rate of proliferation would be that it is involved in the reprogramming of cells fated to become mesoderm and endoderm. Elucidation of the molecular basis of cell cycle control and the way in which growth regulation is integrated with development should help elucidate the mechanisms of differentiation during gastrulation and indicate whether growth is simply a target of developmental regulation or if growth rate can influence developmental decisions.

Cell cycle regulation: A developmental leitmotif or theme with free improvisations?

Our description of the alterations in cell cycle structure in rat embryos demonstrates that the length and structure of the cell cycle are regulated during development in all species examined so far and thus regulation of these aspects of the cell cycle appears to be a common theme of embryogenesis. In *Xenopus* and *Drosophila* development, the cell cycle progresses from very rapid, alternating S and M phases to slower, more complex cycles by adding G_1 and G_2 phases. In rodents the early cycles are relatively slow, followed by a dramatic increase in the rate of proliferation during gastrulation and then slowing as the adult pattern emerges. Even the most rapid cell cycles in the rodent embryo are relatively slow in comparison with the rapid S/M cycles in *Xenopus* and *Drosophila*. It is likely that the mechanisms used to regulate cell cycles during rodent gastrulation are different from those used in early *Xenopus* or *Drosophila* development, despite the superficial similarities of structure. It seems that developmental regulation of cell cycle structure is a robust mechanism to achieve the integration of growth and differentiation during embryogenesis that has been adapted to fit the needs of various organisms.

We thank Jon Cooper (Fred Hutchinson Cancer Research Center) in whose lab this work was started, and whose support and input were invaluable. Many thanks also to Drs Caroline Alexander and David Morgan for their critical reading of the manuscript, Anthony Dayton for his work on the flow cytometer, Sally Little for her help and insight, and Julie (Sunshine) Pascoe-Mason, Leanne Cornel and Barb Doggett for technical assistance. This work was supported by grants from the National Institutes of Health (HD 16287 and HD 22095 to P. Mirkes, HD 26732 and HD 23539 to Z. Werb), and by the US Department of Energy, Office of Health and Environmental Research (contract no. DE-AC03-76-SF01012).

REFERENCES

Arora, K. and Nusslein-Volhard, C. (1992). Altered mitotic domains reveal fate map changes in Drosophila embryos mutant for zygotic dorsoventral patterning genes. *Development* **114**, 1003-1024.

Blumenthal, A. F., Kriegstein, H. J. and Hogness, D. S. (1974). The units of DNA replication in Drosophila melanogaster chromosomes. *Cold Spring Harbor Symposium of Quantitative Biology* **38**, 205-223.

Bolton, V. N., Oades, P. J. and Johnson, M. H. (1984). The relationship between cleavage, DNA replication, and gene expression in the mouse 2-cell embryo. *J. Embryol. Exp. Morph.* **79**, 139-163.

Cikes, M. (1970). Relationship between growth rate, cell volume, cell cycle kinetics, and antigenic properties of cultured murine lymphoma cells. *J. Natl. Cancer Inst.* **45**, 979-988.

Cross, F., Roberts, J. and Weintraub, H. (1989). Simple and complex cell cycles. *Annu. Rev. Cell Biol.* **5**, 341-396.

Dasso, M. and Newport, J. W. (1990). Completion of DNA replication is

monitored by a feedback system that controls the initiation of mitosis in vitro: studies in Xenopus. *Cell* **61**, 811-823.

Downes, C. S., Musk, S. R. R., Watson, J. V. and Johnson, R. T. (1990). Caffeine overcomes a restriction point associated with DNA replication, but does not accelerate mitosis. *J. Cell Biol.* **110**, 1855-1859.

Edgar, B. A. and O'Farrell, P. H. (1989). Genetic control of cell division patterns in the Drosophila embryo. *Cell* **57**, 177-187.

Edgar, B. A. and O'Farrell, P. H. (1990). The three postblastoderm cell cycles of Drosophila embryogenesis are regulated in G_2 by string. *Cell* **62**, 469-480.

Foe, V. E. (1989). Mitotic domains reveal early commitment of cells in Drosophila embryos. *Development* **107**, 1-22.

Foe, V. E. and Odell, G. (1989). Mitotic domains partition fly embryos, reflecting early cell biological consequences of determination in progress. *Amer. Zool.* **29**, 617-652.

Fujinaga, M. and Baden, J. M. (1991). A new method for explanting early postimplantation rat embryos for culture. *Teratology* **43,** 95-100.

Glover, D. M. (1991). Mitosis in the Drosophila embryo - in and out of control. *Trends Genet.* **7**, 125-132.

Graham, C. F. and Morgan, R. W. (1966). Changes in the cell cycle during early amphibian development. *Dev. Biol.* **14**, 439-460.

Hartwell, L. H. and Smith, D. (1985). Altered fidelity of mitotic chromosome transmission in cell cycle mutants of S. cerevisiae. *Genetics* **110**, 381-395.

Hartwell, L. H. and Weinert T. (1989). Checkpoints: controls that ensure the order of cell cycle events. *Science* **246**, 629-634.

Hittelman, W. N. and Rao, P. N. (1974a). Bleomycin-induced damage in prematurely condensed chromosomes and its relationship to cell cycle progression in CHO cells. *Cancer Res.* **34**, 3433-3439.

Hittelman, W. N. and Rao, P. N. (1974b). Premature chromosome condensation 1: visualization of X-ray-induced chromosome damage in interphase cells. *Mutation Res.* **23**, 251-258.

Howlett, S. K. (1986). A set of proteins showing cell cycle dependent modification in the early mouse embryo. *Cell* **45**, 387-396.

Howlett, S. K. and Bolton, V. N. (1985). Sequence and regulation of morphological and molecular events during the first cell cycle of mouse embryogenesis. *J. Embryol. Exp. Morph.* **87**, 175-206.

Kauffman, S. L. (1968). Lengthening of the generation cycle during embryonic differentiation of the mouse neural tube. *Exp. Cell Res.* **49**, 420-424.

Kimelman, D., Kirschner, M. W. and Scherson, T. (1987). The events of midblastula transition in Xenopus are regulated by changes in the cell cycle. *Cell* **48**, 399-407.

Kung, A. L., Zetterberg, A., Sherwood, S. W. and Schimke, R. T. (1990). Cytotoxic effects of the cell cycle phase specific agents: result of cell cycle perturbation. *Cancer Res.* **50**, 7307-7317.

Lau, C. C. and Pardee, A. B. (1982). Mechanism by which caffeine potentites lethality of nitrogen mustard. *Proc. Natl. Acad. Sci. USA* **79,** 2942-2946.

Lawson, K. A., Pedersen, R. A. and Van der Geer, S. (1987). Cell fate, morphogenetic movement and population kinetics of embryonic endoderm at the time of germ layer formation in the mouse. *Development* **101**, 627-652.

Lawson, K. A., Meneses, J. J. and Pedersen, R. A. (1991). Clonal analysis of epiblast fate during germ layer formation in the mouse embryo. *Development* **113**, 891-911.

Lewis, N. E. and Rossant, J. (1982). Mechanism of size regulation in mouse embryo aggregates. *J. Embryol. Exp. Morph.* **72**, 169-181.

Loeffler, M., Stein, R., Wichmann, H. E., Potten, C. S., Kaur, P. and Chwalinski, S. (1986). Intestinal cell proliferation. 1. A comprehensive model of steady-state proliferation in the crypt. *Cell Tiss. Kin.* **19**, 627-645.

Luthardt, F, W. and Donahue, R. P. (1975). DNA synthesis in developing two-cell mouse embryos. *Dev. Biol.* **44**, 210-216.

McKnight, S. L. and Miller, O. L. (1977). Electron microscopic analysis of chromatin replication in the cellular blastoderm Drosophila melanogaster embryo. *Cell* **12**, 795-804.

Minden, J. S., Agard, D. A., Sedat, J. W. and Alberts, B. M. (1989). Direct cell lineage analysis in Drosophila melanogaster by time-lapse, three-dimensional optical microscopy of living embryos. *J. Cell Biol.* **109**, 505-516.

Mirkes, P. E., Ricks, J. L. and Pascoe-Mason, J. M. (1989). Cell cycle analysis in the cardiac and neurepithelial tissues of day 10 rat embryos and the effects of phosphoramide mustard, the major teratogenic metabolite of cyclophosphamide. *Teratology* **39**, 115-120.

Newport, J. and Kirschner, M. (1982). A major developmental transition in early Xenopus embryos: 1- Characterization and timing of cellular changes at the midblastula stage. *Cell* **30**, 675-686.

Niswander, L. and Martin, G. R. (1992). Fgf-4 expression during gastrulation, myogenesis, limb and tooth development in the mouse. *Development* **114**, 755-768.

O'Farrell, P. H., Edgar, B. A., Lakich, D. and Lehner, C. F. (1989). Directing cell division during development. *Science* **246**, 635-640.

Pardee, A. B. (1989). G_1 events and regulation of cell proliferation. *Science* **246**, 603-608.

Poelmann, R. E. (1981). Differential mitosis and degeneration patterns in relation to the alterations in the shape of the embryonic ectoderm of early post-implantation mouse embryos. *J. Embryol. Exp. Morph.* **55**, 33-51.

Potten, C. S. and Loeffler, M. (1990). Stem cells: attributes, cycles, spirals, pitfalls and uncertainties. Lessons for and from the crypt. *Development* **110**, 1001-1020.

Rabinowitz, M. (1941). Studies on the cytology and the early embryology of the egg of Drosophila melanogaster. *J. Morph.* **69**, 1-49.

Raff, J. W. and Glover, D. M. (1988). Nuclear and cytoplasmic mitotic cycles continue in Drosophila embryos in which DNA synthesis is inhibited with aphidicolin. *Dev. Biol.* **107**, 2009-2019.

Rappolee, D. A., Sturm, K. S., Behrendtsen, O., Schultz, G. A., Pedersen, R.A. and Werb, Z. (1992). Insulin-like growth factor ll acts through an endogenous growth pathway regulated by imprinting in early mouse embryos. *Genes Dev.* **6**, 939-952.

Russell, P. and Nurse, P. (1986). $cdc25^+$ functions as an inducer in the mitotic control of fission yeast. *Cell* **45**, 145-153.

Sawicki, W., Abramczuk, J. and Blaton, O. (1978). DNA synthesis in the second and third cell cycles of mouse preimplantation development. *Exp. Cell Res.* **112**, 199-205.

Snow, M. H. L. (1977). Gastrulation in the mouse: growth and regionalization of the epiblast. *J. Embryol. Exp. Morph.* **42**, 293-303.

Solter, D., Skreb, N. and Damjanov, I. (1971). Cell cycle analysis in the mouse egg-cyclinder. *Exp. Cell Res.* **64**, 331-334.

Sullivan, W., Minden, J. S. and Alberts, B. M. (1990). daughterless-abo-like, a Drosophila maternal-effect mutation that exhibits abnormal centrosome separation during the late blastoderm divisions. *Development* **110**, 311-323.

Tobey, R. A. (1975). Different drugs arrest cells at a number of distinct stages in G_2. *Nature* **254**, 245-247.

Tobey, R. A., Anderson, E. C. and Petersen, D. F. (1967). The effect of thymidine on the duration of G_1 in Chinese Hamster cells. *J. Cell Biol.* **35**, 53-59.

Weinert, T. A. and Hartwell, L. H. (1988). The RAD9 gene controls the cell cycle response to DNA damage in Saccharomyces cerevisiae. *Science* **241**, 317-322.

(Accepted 26 November 1992)